Journal of Applied Sciences

ISSN 1812-5654

science alert

ANSInet
an open access publisher
http://ansinet.com

Journal of Applied Sciences 8 (1): 59-67, 2008
ISSN 1812-5654

Use of a Component with Fractional Impedance in the Realization of an Analogical Regulator of Order ½

[1]T. Cisse Haba, [1]Georges L. Loum, [1]Jérémie T. Zoueu and [2]G. Ablart
[1]INP-HB, Département Génie Electrique et Electronique, BP 1093 Yamoussoukro, Côte d'Ivoire
[2]LGET, University Paul Sabatier Bât.III R1b2, 118 Route de Narbonne, F-31062 Toulouse Cedex, France

Abstract: The objective of this study is to show the best stability of a regulation system using a nonconventional corrector like that carried out compared to system of regulation using a traditional corrector. The input impedance of the electronic component realized has a fractional order in a frequency band called fractal area. This property suggests their use in the practical realization of analogical controllers of a non-integer nature. In this article, a fractional controller of order ½ is realized by using an electronic component based on the fractal structure of Hilbert. Some simulations and experiments have demonstrated that the proposed component is useful for the realization of ½ order fractional controller.

Key words: Fractal, electronic component, fractional controller

INTRODUCTION

In a number of previous studies, control systems, based on fractional order correctors and using theoretical methods, have been depicted. Those mathematical analyses have brought to the fore, the better performances of control system using $PI^{\lambda}D^{\mu}$ (proportional Integral Derivative with fractional order). Here, λ and μ are non-integer order; as opposed to systems using the basics types of PID with integer order. These research works, especially those of Joaquin *et al.* (2006) have proved the systems using the new types of correctors to be more robust and interference free.

Our findings are to emphasize the above. In other words, our results, one more, have practically confirmed the better performance exhibited by the feedback system, applied to a capacitive structure (Haba *et al.*, 1997, 2005) with fractional order impedance. The experiments done on those structures have helped showing that they have, over a certain range of frequencies, an input impedance whose modulus is of the form $|Z| \propto (i\omega)^{-\eta}$. Where η is a fractional and θ a constant argument of the form $\theta = -\eta x \pi/2$.

This useful property will be used in this study, for the making up of fractional correctors whose usefulness has been brought out by the works of Oustaloup (1999), on the Non-Integer Order and Robust Command (NIORC).

Some studies like those of Le Méhauté and Crepy (1983) once again highlights the interest of these structures in electric circuits. They bring forward the concept of fractance which is a new kind of electric circuit with intermediate properties, between those of resistance and capacitances. These new type of circuits have experimentally been tested by Oldham and Zoski (1983), Nakagawa and Sorimachi (1992) as well as by Yifei *et al.* (2005). In this study, we are going to look at the fractional correctors of ½ orders, which are in fact, electronic devices having a purely capacitive structure with Hilbert Fractional impedance.

HILBERT'S FRACTAL STRUCTURE COMPONENT DESIGN

The fractal structures are geometrical shapes that are obtained by an iterative process (Le Méhauté, 1990; Gouyet, 1992). Hilbert's is obtained starting from an initiator pattern (« 0 » iteration structure), square shaped having one its sides deleted (Fig. 1). Each remaining side is of length L. On the four initiator pattern peaks, N = 4 square shapes identical to the initial squares, but reduced in length by a factor $\alpha = 2$ are constructed. These new squares are centred on the peaks of the initiator square before being interconnected by segments of length L/α.

The structure obtained in this way at iteration 1, constitutes the fractal structure generator pattern.

To advance to the next higher iteration level, the principle of the previous generation is applied to all the elementary squares of the current iteration. The knowledge of the reduction factor α and of the number N

Corresponding Author: T. Cisse Haba, INP-HB, Département Génie Electrique et Electronique, BP 1093 Yamoussoukro (RCI), Côte d'Ivoire Tel: 00 (225) 07 84 20 00

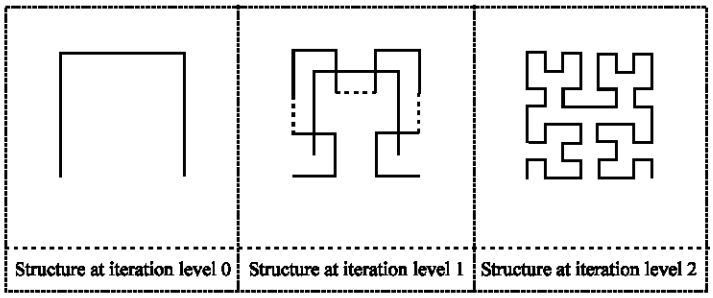

Fig. 1: The generation process of Hilbert's fractal structure

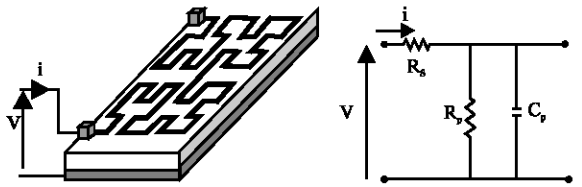

Fig. 2: Hilbert's fractal structure component and its equivalent electrical layout

of squares created at each iteration, permits to determine the fractal dimension of the structure using Eq. 1. In this the Hilbert fractal structure has as a fractal dimension of 2.

$$D_f = \frac{Log(N)}{Log(\alpha)} \quad (1)$$

The electronic component is manufactured by a micro-electronic process. Each component (Fig. 2) can be considered as a Metal-Oxide-Semiconductor (MOS) capacitor. One of the capacitor plates is made up of a silicon substrate. The fractal pattern transfer on this plate is obtained by photolithography. On the back side of the other plate, a fine aluminium layer is deposited in order to constitute the electrical ground level. The two plates are separated by the silicon oxide (SiO_2) which is an insulator. The contact studs are planned to permit an interconnection with the test circuit by micro-soldering.

From an electric point of view, each elementary segment of the fractal pattern can be modelled by a cell of the $R_sC_pR_p$ type of cell (Fig. 2). R_s and C_P characterize the resistance and the capacity of the semiconductor bar. The leakage resistance R_P in parallel with C_P, permits to account for the grid oxide quality. We have shown that this model is quite suitable to describe our component behaviour (Haba *et al.*, 2005).

COMPONENT BEHAVIOR AS A FUNCTION OF FREQUENCY

The tests carried out on the component under study permitted to obtain the curves shown in Fig. 3 which show the variations in the modulus and the phase of the input impedance of the component in the 10 Hz at 10^6 Hz frequency band. These curves are plotted on a semi-logarithmic scale.

As we can perceive, our Hilbert fractal structure component is characterized by complex input impedance which possesses a constant phase within a given frequency band that we term fractal zone. The Constant Phase Angle (CPA) has a value of -45° and the fractal zone extends from approximately from 2.10^2 Hz to 10^6 Hz.

This zone is also characterized by a decrease in input impedance modulus following to a negative fractal order slopes η. This slope of -0.499 is very close to -0.5. Also, we can establish in the fractal zone, the expression for the input impedance $Z_i(j\omega)$ of our component in which B is a constant that one can easily determine from the input impedance modulus plot:

$$Z_e(j\omega) = B \times (j\omega)^{-0,5} \Leftrightarrow \begin{cases} |Z_e(j\omega)| = \frac{B}{\sqrt{\omega}} = \frac{1.6.10^6}{\sqrt{\omega}} \\ Arg(Z_e(j\omega)) = -45° \end{cases} \quad (2)$$

This result is interesting in case, within the fractal zone, the input impedance expression of our component is very simple and that the argument of this impedance has a constant value equal to -45°. These characteristics can be put to advantage in the design of certain circuits such as analogic controllers. Indeed, our component of fractional impedance of order 1/2 can serve to advance by 45° the phase of an insufficiently stable process, in order to ensure a comfortable stability for it along with offering it a good compromise between the initial rapidity and the stabilization speed.

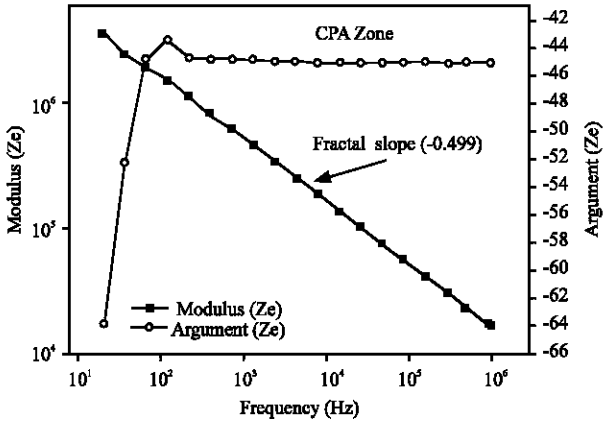

Fig. 3: Modulus and argument of the Hilbert's fractal structure component-input impedance Z_e

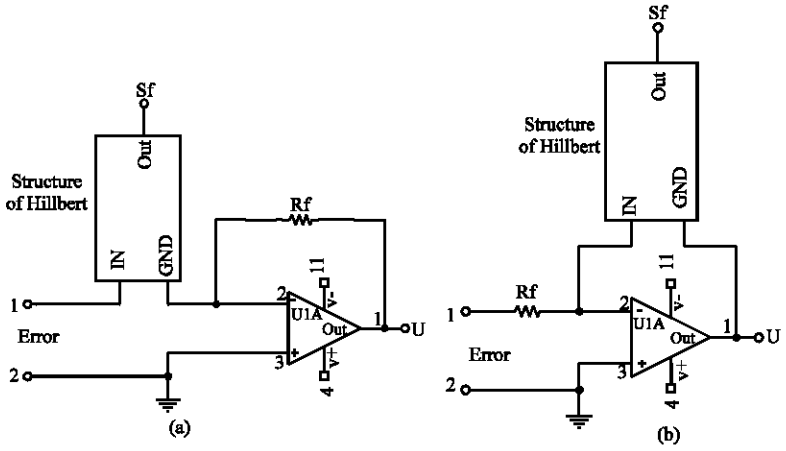

Fig. 4: Derivative (a) and integrator (b) circuits realized with the Hilbert's fractal structure component

The circuits of Fig. 4 are those of a differentiator and an integrator of order 1/2 realized with our component. This is electrically symbolized by a-3 terminals block. The input impedance is measured between input and ground terminals. The ouput terminal S_f puts the component in cascade with another.

If $Z_e(p)$ denotes the operational impedance of our component, the circuit transfer functions of the Fig. 4 are respectively:

$$C_{PDF}(p) = \frac{R_f}{Z_e(p)} = \frac{R_f}{B} \cdot \sqrt{p} \quad (3)$$

$$C_{PIF}(p) = \frac{B}{R_f \sqrt{p}} \quad (4)$$

These transfer functions are those of fractal order controllers whose importance was highlighted by Oustaloup (1999) in his approach to CRONE. As a matter of fact, contrary to the conventional controllers whose phase advance varies with the process gain, that of the fractal order controller is theoretically constant. This ensures a degree of strong stability with in relation to the gain variation.

In previous study, we looked at how these silicon structures could be used to make electronic devices embedded in a case, for their characterization. After that the electrical modeling was completed, we investigated the behavior of the input impedance of these structures with non-integer dimension. This allowed us to point out their specific characteristics, when comparing them to those with integer structure.

In addition, we were interested in the influence of the R_s, C_P and R_P parameters of the electrical model. This was done over the interval with fractional slope and Constant Phase Angle (CPA).

In the present study, we are going to focus on how these electronics devices can be used in the field of control engineering, for optimal stability improvement.

Our objective in what follows, is to bring into evidence the possibility of realizing fractional order controllers with our component. The performances of this type of controller will be on the one hand, compared with the conventional controllers and on the other hand, analyzed from the point of view of the robustness with respect to the gain variation. To do that, we will present initially, the results of simulation obtained during PD and PI of corrections process, ahead of the experimental results that we programmed during a PI correction integrating our fractal structure component.

IMPLEMENTATION OF FRACTIONAL CONTROLLERS

The functional diagram of the servo-system that we would study is shown in Fig. 5, where V_p represents an external interference entering the servo-system.

Proportional and Derivative (PD) based correction: In this part, we presume that $V_p = 0$ and that the process transfer function corresponds to that of a double integrator:

$$G(p) = \frac{A}{p^2}.$$

This process is at the limit of stability. The objective is to render it stable by intending a series correction. The Open Loop Transfer Function (OLTF) of the corrected system is: C(p)×G(p).

The standard PD controller utilized to improve the phase margin is the phase advanced controller whose transfer function has an expression:

$$C_{PDC}(p) = k_1 \frac{1+aTp}{1+Tp} \quad \text{With } a>1 \qquad (5)$$

This controller (PDC) brings to the system a phase advance

$$\Delta\varphi = \arcsin\frac{a-1}{a+1},$$

which depends on the cut-off angular frequency ω_{C0} and thus on the open loop system gain.

The fractional PDF controller that we propose, guarantees the system a phase advance of 45° independent of the magnitude of gain. Its transfer function can be put under the form:

$$C_{PDF}(p) = k_2\sqrt{p} \quad \text{with } k_2 = \frac{R_f}{B} \text{ and } B = 1.6.10^6 \qquad (6)$$

In order to simulate these two different corrections, the analogue circuits have been realized in Fig. 6.

At the start, the controllers have been synthesized so that their step response is near identical for the nominal adjustment i.e. the open loop gain K of the corrected system is equal to 1, at the cut off angular frequency ω_{C0}.

The Table 1 regroups the results determining each circuit component for the nominal adjustment, fixing ω_{C0} with 25132 rad sec^{-1} (f_0 = 4 Khz) and researching for a phase margin $\Delta\phi$ = 45°.

The step response of each of the two servo-systems is given in Fig. 7 for different values of K: 0.21, 1 and 5.

We remark that the over-run of the step response of the system provided with a standard PD controller is variable and increases with the gain K, which is translated results into system stability decay with the rise in gain K. On the opposite case, for the fractional PD controller, the step response conserves the same overshoot. The fact that the step response in the case of the fractional PD controller retains the same shape with varying gain means that the degree of stability is maintained i.e., the phase margin. The corrected system is thus robust related to the gain variation. However, we remark a time-axis expansion with rising K. In other words, the rise-times are more important with the fractional PD controller.

Proportional and Integral (PI) based correction: In the functional diagram of Fig. 5, C(p) is actually a PI controller and the process transfer function is now:

$$G(p) = \frac{1}{Tp}.$$

The conventional PI controllers and fractional PI controllers that we would use of in our simulation, have the following transfer functions:

$$C_{PIC}(p) = k_3 \cdot \frac{1+T_i p}{T_i p} \text{ and } C_{PIF}(p) = \frac{k_4}{\sqrt{p}} \qquad (8)$$

The principal objective of the servo-system is to make the output voltage Vs follow up the input consigned

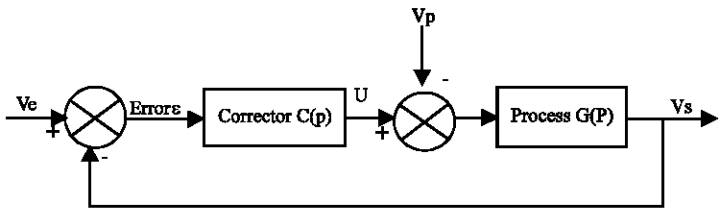

Fig. 5: Block diagram of the servo-system under study

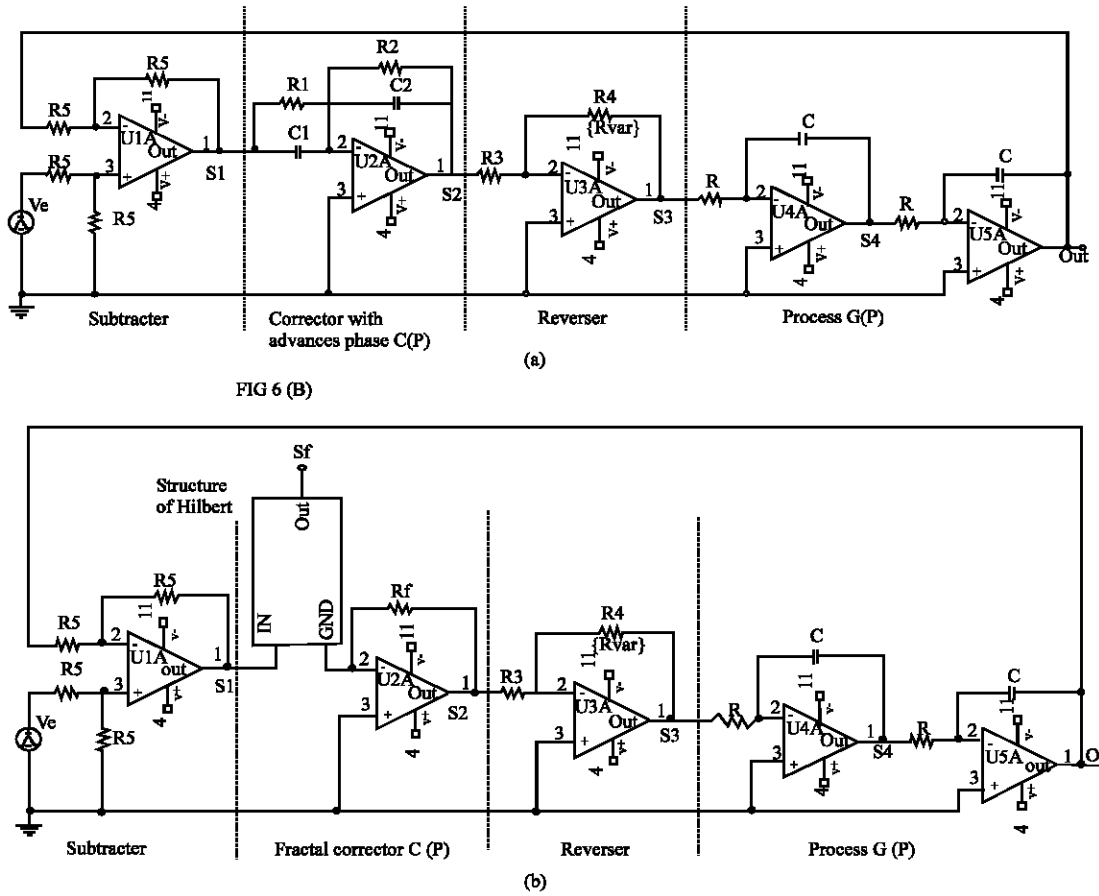

Fig. 6: PD Correction: (a) conventional and (b) fractional

Table 1: Synthesis of the correctors proportional derivative and proportional fractional derivative

System settings	Traditional corrector PD (PDC)	Fractional corrector PD (PDF)
Process transfer function	$G(p)=\frac{A}{p^2}$	
Desired performances	$\omega_{c0}=25132$ rad sec^{-1} and $\Delta\varphi=45°$ with $\lvert C(j\omega_{c0})G(j\omega_{c0})\rvert = 1$	
Data	$R=1$ kΩ; $C=0.1$ µF; $R_1=R_3=R_4=R_5=5$ kΩ	
Transfer function in open loop of the corrected system	$k_1\frac{A(1+aTp)}{p^2(1+Tp)}$	$k_2\frac{A\sqrt{p}}{p^2}$
Calculation of components	$A=\frac{1}{(RC)^2}\Rightarrow A=10^6$	
	$\Delta\varphi=45° \Rightarrow a=5.8$	
	$T=\frac{1}{\omega_{c0}\sqrt{a}}\Rightarrow T=16.5$ µsec	
	$k_1=\frac{\omega_{c0}^2}{A\sqrt{a}}\Rightarrow k_1=2.62$	$A=\frac{1}{(RC)^2}\Rightarrow A=10^6$
	$R_2=k_1R_1\Rightarrow R_2=13.1$ kΩ	$k_2=\frac{\omega_{c0}^{3/2}}{A}\Rightarrow k_2=0.04$
	$C_1=\frac{T}{R_2}\Rightarrow C_1=1.26$ nF	$R_f=1.6\times10^6 k_2\Rightarrow R_f=63.6$ kΩ
	$C_1=\frac{aR_2C_2}{R_1}\Rightarrow C_1=19$ nF	

or referenced voltage V_e. It is thus a voltage follow-up for which can arise certain tracking (follow-up of the directive without any disturbance) or control (rejection of voltage interference) problems. We are interested in the first place in tracking problem ($V_p = 0$). The electrical circuits realized for our different servo-systems are indicated in Fig. 8.

The conventional PI controller parameter determination was carried out by referring the servo-

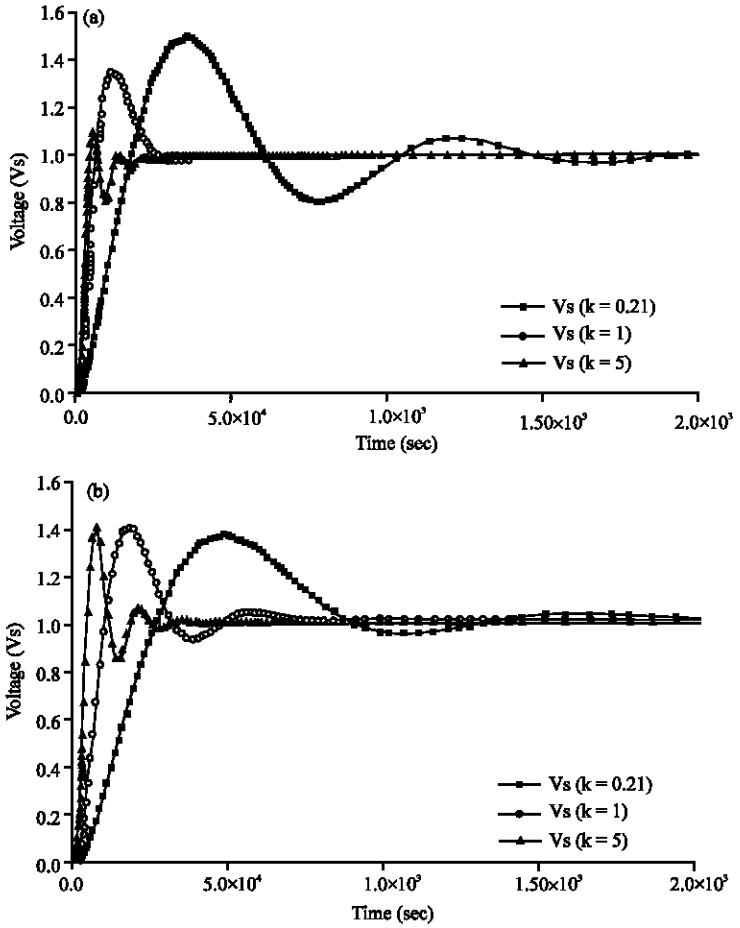

Fig. 7: Variable gain Step function of the servo-system: (a) conventional controller PD and (b) fractional PD controller

Table 2: Synthesis of the correctors proportional fractional integral and proportional integral

System settings	Traditional corrector PI (PIC)	Fractional corrector PI (PIF)
Process transfer function	$G(p)=\frac{1}{Tp}$	
Desired performances	$\omega_n = 25132$ rad sec^{-1}; $\xi = 0.7$ with $\lvert C(j\omega_n)\,G(j\omega_n)\rvert = 1$	
Data	R = 1kΩ; C = 0.1 µF; R_1 = 5kΩ	
Transfer function of tracking (V_p = 0)		
	Transfer function in loop closed	Transfer function in loop open
	$FTBF=\frac{A(1+T_1p)}{\frac{TT_1}{k_3}p^3+T_1p+1}$	$FTBO=\frac{k_4}{Tp^{3/2}}$
Calculation of components	T = Rc ⇒ T = 100 µsec	
	$R_i=\frac{T_1}{C_1}\Rightarrow Ri=5.6\ k\Omega$	T = Rc ⇒ T = 100 µsec
	$T_1=\frac{2\xi}{\omega_n}\Rightarrow Ti=56\ \mu sec$	$k_4=T\omega_n^{3/2}\Rightarrow k4=398.5$
	$k_3=TT_1\omega_n^2\Rightarrow k3=3.52$	
	$R_c=\frac{R_i}{k_3}\Rightarrow Rc=1.6\ k\Omega$	$R_f=\frac{B}{k_4}\Rightarrow R_f=4\ k\Omega$

system to a second order system having a natural angular frequency ω_n = 25132 rad sec^{-1} and a damping coefficient ξ = 0.7. These values guarantee a minimal response time and a sufficient stability margin of 45°. For the PI fractional controller, the nominal adjustment has been realized for $\omega_{CO} = \omega_n$ = 25132 rad sec^{-1}. The different PI correction circuit component values obtained under the created conditions are available in Table 2.

The follow-up simulation plots are represented on Fig. 9, for different values of the capacitance C which

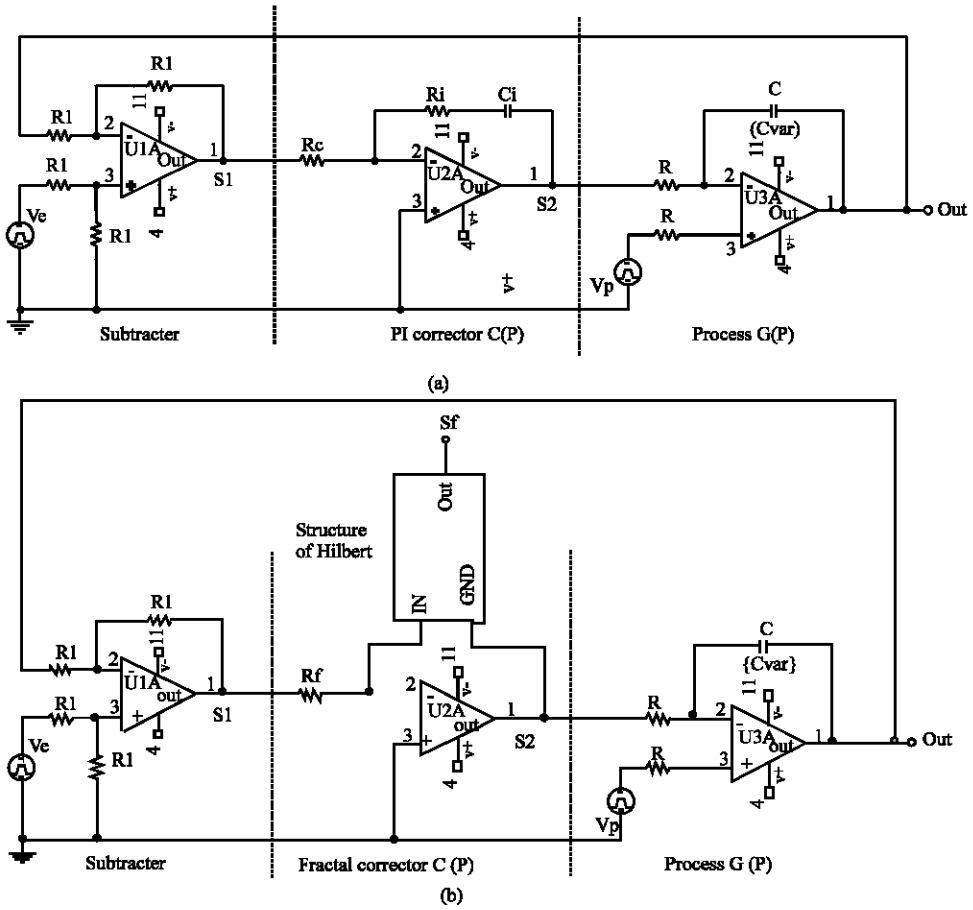

Fig. 8: PI correction: (a) conventional and (b) fractional

permits to adjust the open loop gain. We remark that the gain variations do not affect the overshoot of different step responses concerning the fractional correction. Moreover, the pseudo-oscillatory regime is practically inexistent. In the case of the conventional PI controller on the other hand, the indexed response oscillations are clear and overshoots vary greatly with the gain. The degree of stability is thus weak for certain values of K.

It is equally important to indicate that in both cases, the position static error is null. The static precision is thus satisfactory. Moreover, in the two cases, the steady state operation is attained all the more rapidly as the gain decays. However, the PI fractional controller permits to attain this regime more rapidly with a better response of the system.

We have also recorded (Fig. 10) the responses of the two servo-systems in the presence of a step disturbance V_p, shifted in time with respect to a consigned constant step voltage.

The rejector behaviour of the two systems facing disturbances is clearly visible. However, as it was to expect, the disturbance rejection of the fractional PI controller leaves a trail caused by the fractional controller order. Indeed, the signal recovery is slower in the case of an integrator of order 1/2 than of an integrator of the order 1 because of the memory effect.

Practical implementation of our component in a PI correction: The results obtained during simulations motivated us to put into practice a PI correction provided with a fractal structure component. The Fig. 11 presents our circuit representing fractional PI controller. The oscillograms readings are shown in Fig. 12.

We ascertain that the experimental results correspond to those of simulation:

- In the follow-up, the system response time is reduced, the oscillations are rapidly damped and the static precision is good.
- In regulation, we assist to the rejection of the disturbances with, however, a remarkable trail.

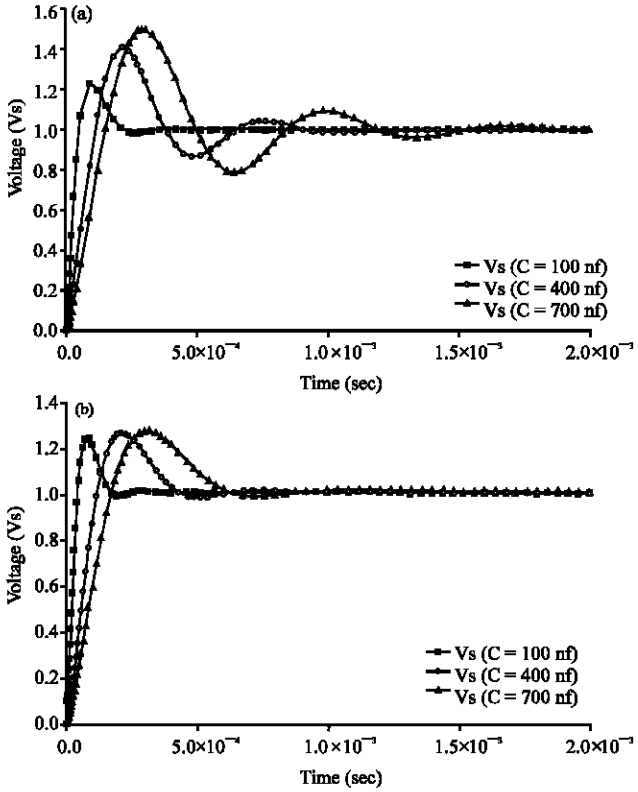

Fig. 9: Step function response in servo-system follow-up: (a) conventional PI controller and (b) fractional PI controller

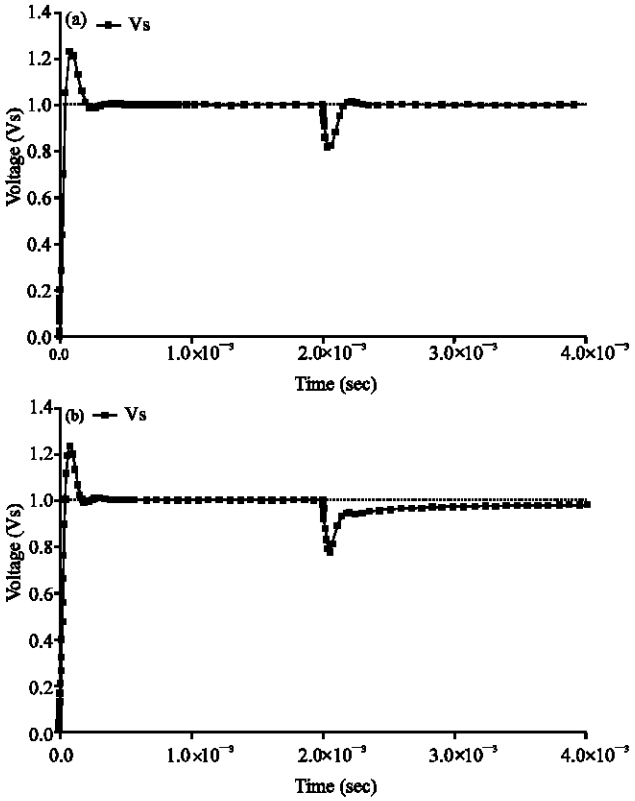

Fig. 10: Step-function response in servo-system regulation: (a) conventional PI controller and (b) fractional PI controller

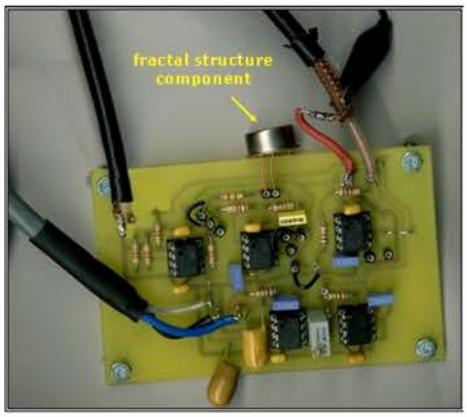

Fig. 11: Fractional PI controller circuit design

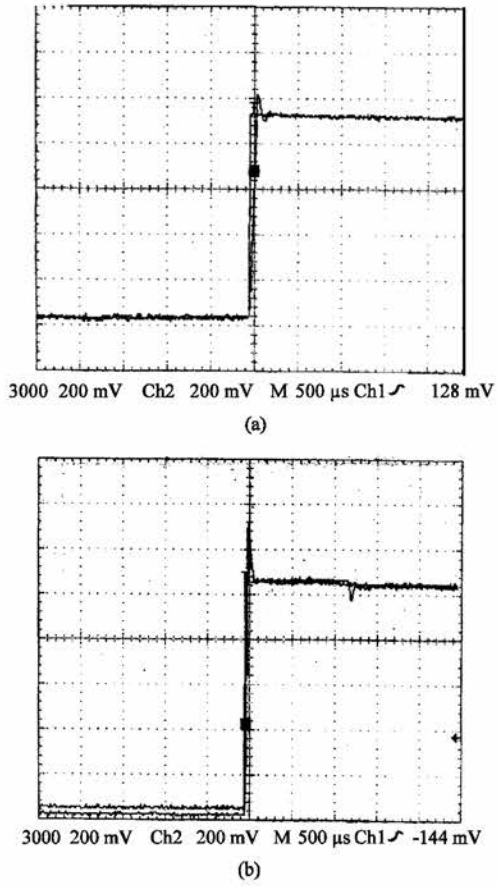

Fig. 12: (a) Real time step-function response of the servo-system follow-up and (b) regulation (y-axis: The magnitude of the output signal Vs)

CONCLUSIONS

We have shown in this article which our Hilbert fractal electronic component presents a fractional impedance of order 1/2 that we profitably implemented in the design of proportional derivative and proportional integral fractional controllers. The simulations and experiments carried out have demonstrated that the fractional controllers equipped with our fractal structure component permitted:

- In PD correction, to ensure an adequate degree of stability independent of the value of open loop gain.
- In PI correction, to obtain a perfect static precision in follow-up and a light trail in regulation.

These results, characteristic to the fractional controllers, indicate that the utilization of our Hilbert-fractal structure component which presents the advantage of being easily obtained using micro-electronic process, is convenient for the realization of a fractional controller of order 1/2.

REFERENCES

Gouyet, J.F., 1992. Physique et Structures Fractales. Edition Masson, Paris, Milan, Barcelone, Bonn.

Haba, T.C., G. Ablart and T. Camps, 1997. The frequency response of a fractal photolithographic structure. IEEE. Trans. Dielectrics and Electrical Insulation, 4 (3): 321-326.

Haba, T.C., G. Ablart, T. Camps and F. Olivie, 2005. Influence of electrical parameters on the input impedance of a fractal structure realised on silicon. Chaos, Solitons and Fractals, 24: 479-490.

Joaquin, C., B. Alfonso, A.C. Monje and V.M. Blas, 2006. Tuning of fractional PID controllers by using QFT. IEEE Industrial Electronics, IECON-32nd Annual Conference on Nov., pp: 5402-5407.

Le Méhauté, A. and G. Crepy, 1983. Introduction to transfer and motion in fractal media: The geometry of kynetics. Solid State Ionics, 9-10: 17-30.

Le Méhauté, A., 1990. Les géométries fractales. Hermes, Paris.

Nakagawa, M. and K. Sorimachi, 1992. Basic characteristics of a fractance device. IEICE. Trans. Fundam., E75-A (12): 1814-1819.

Oldham, K.B. and C.G. Zoski, 1983. Analogue instrumentation for processing polarographic data. J. Electroanal. Chem., 157 (1): 27-51.

Oustaloup, A., 1999. La Commande CRONE du Scalaire au Multivariable. 2nd Edn. Revue et Augmentée, Edition Hermès Science Publications, Paris.

Yifei, P., Y. Xiao, L. Ke, Z. Jiliu, Z. Ni, Z. Yi and P. Xiaoxian, 2005. Structuring analog fractance circuit for 1/2 order fractional calculus. ASICON. 6th International Conference on ASIC, 2: 1136-1139.